

## NON-EXTENSIVE STATISTICAL EFFECTS IN NUCLEAR MANY-BODY PROBLEMS

A. LAVAGNO<sup>1</sup>, P. QUARATI<sup>2</sup>

<sup>1</sup>*Dip. di Fisica, Politecnico di Torino and INFN Sezione di Torino, Italy*

<sup>2</sup>*Dip. di Fisica, Politecnico di Torino and INFN Sezione di Cagliari, Italy*

(Received June 20, 2007)

*Abstract.* Density and temperature conditions in many stellar core and in the first stage of relativistic heavy-ion collisions imply the presence of non-ideal plasma effects with memory and long-range interactions between particles. Recent progress in statistical mechanics indicates that Tsallis non-extensive thermostatics could be the natural generalization of the standard classical and quantum statistics, when memory effects and long range forces are not negligible. In this framework, we show that in weakly non-ideal plasma non-extensive effects should be taken into account to derive the equilibrium distribution functions, the quantum fluctuations and correlations between the particles. The strong influence of these effects is discussed in the context of the solar plasma physics and in the high-energy nuclear-nuclear collision experiments. Although the deviation from Boltzmann-Gibbs statistics, in both cases, is very small, the stellar plasma and the hadronic gas are strongly influenced by the non-extensive feature and the discrepancies between experimental data and theoretical previsions are sensibly reduced.

*Key words:* nuclear astrophysics, relativistic heavy-ion collisions.

### 1. INTRODUCTION

We wish to discuss two applications of the non-extensive statistics (NES) concerning the evaluation of:

- metastable state and random electric microfields in dense stellar plasma;
- non-ideal plasma effects and rapidity distribution in relativistic heavy-ion collisions.

In both applications a very small deviation from standard statistics gives rise to sensible and important changes of several average physical observables, with a clear and wide reduction of the disagreement with the experimental results, evident when standard statistics is assumed.

### 2. NUCLEAR ASTROPHYSICS

The solar core is a neutral system of electron, protons, alpha particles and other heavier nuclei, usually assumed as an ideal plasma in thermodynamical

equilibrium described by a Maxwellian ion velocity distribution. Because the nuclear rates of the most important reactions in stellar core are strongly affected by the high-energy tail of the ion velocity distribution, let us start by reminding the meaning of ideal and non-ideal plasma. A plasma is characterized by the value of the plasma parameter  $\Gamma$

$$\Gamma = \frac{\langle U \rangle_{\text{Coulomb}}}{\langle T \rangle_{\text{thermal}}}, \quad (1)$$

where  $\langle U \rangle_{\text{Coulomb}}$  is the mean Coulomb potential energy and  $\langle T \rangle_{\text{thermal}}$  is the mean kinetic thermal energy. Depending on the value of the plasma parameter we can distinguish three regimes:

- $\Gamma \ll 1$  – Dilute weakly interacting gas, the Debye screening length  $R_D$  is much greater than the average interparticle distance  $r_0 \approx n^{1/3}$ , there is a large number of particles in the Debye sphere.
- $\Gamma \approx 0.1 \div 1$  –  $R_D \approx r_0$ , it is not possible to clearly separate individual and collective degree of freedom and the plasma is a weakly non-ideal plasma.
- $\Gamma \geq 1$  – High-density/low-temperature plasma, Coulomb interaction and quantum effects dominate and determine the structure of the system.

In the solar interior the plasma parameter  $\Gamma_{\odot} \approx 0.1$  and the solar core can be considered as a weakly nonideal plasma. Similar behavior occurs in other astrophysical systems with  $0.1 < \Gamma < 1$ , among the others we quote brown dwarfs, the Jupiter core, stellar atmospheres. Weakly nonideal conditions can influence how the stationary equilibrium can be reached within the plasma.

In fact, in weakly nonideal astrophysical plasmas we have that the collision time is of the same order of magnitude of the mean time between collisions, therefore, several collisions are necessary before the particle loses memory of the initial state; collisions between quasi-particles (ion plus screening cloud) are inelastic and long-range interactions are present.

In the next subsection we will see how the presence of memory and long-range forces can influence the thermodynamical stability and the stationary distribution function inside the stellar core.

## 2.1. METASTABLE STATES OF STELLAR ELECTRON-NUCLEAR PLASMA

We can distinguish two kinds of thermodynamical equilibrium state [1]:

- global thermodynamical equilibrium: the free energy density is minimized globally;
- local thermodynamical equilibrium: free energy density is minimized only in a restricted space, not globally. In this case the system is in a metastable state.

Metastable states are always characterized by long-range interactions and/or fluctuations of intensive quantities (like inverse temperature  $\beta$ , density, chemical potential) and the stationary distribution function can be different from the Maxwellian one. In fact, in many-body long-range-interacting systems, it has been recently observed the emergence of long-standing *quasi stationary (metastable) states* characterized by non-Gaussian velocity distributions, before the Boltzmann-Gibbs equilibrium is attained [2, 3].

Considering the corrections to an ideal gas due to identity of particles and to inter-nuclear interaction and the black-body radiation emitted, by minimizing the free energy density of the electron-nuclear plasma, we have obtained the following values [4]

$$n_* \approx 2.74 \cdot 10^{-14} \text{ fm}^{-3}, \quad k_B T_* \approx 5 \cdot \text{keV} \quad \text{and} \quad R_* \approx 0.2 R_\odot,$$

with a typical stellar chemical composition  $\bar{Z} = 1.25$ . States with different values of  $k_B T$  (lower) and  $n$  (higher) are metastable states that can be featured by temperature fluctuations or density fluctuations, by quasi-particle models or by the presence of self-generated magnetic fields or random microfields distributions.

The values obtained above are more than three times higher than the actual temperature of the solar interior and an electron density about half the actual value in the solar core. Therefore, the core of a star like the Sun can not exactly be considered in a global thermodynamical equilibrium state but can be better described as a metastable state and the stationary distribution function could be slightly different from the Maxwellian distribution.

In this context, it has been shown that when many-body long-range interactions are present, in many cases the system exhibits stationary metastable properties with power law distribution well described within the Tsallis nonextensive thermostatistics [5, 6, 7].

## 2.2. MICROSCOPIC INTERPRETATION: RANDOM ELECTRICAL MICROFIELD

In this section we want to investigate about a microscopic justification of a metastable power-law stationary distribution inside a stellar core. At this scope, let us start by observing that the time-spatial fluctuations in the particles positions produce specific fluctuations of the microscopic electric field (with energy density of the order of  $10^{-16} \text{ MeV/fm}^3$ ) in a given point of the plasma. These microfields have in general long-time and long-range correlations and can generate anomalous diffusion. The presence of the electric microfield average energy density,  $\langle E^2 \rangle$ , modifies the stationary solution of the Fokker-Planck equation and the ion equilibrium distribution can be written as

$$f(v) = C \exp \left\{ - \int_0^v \frac{mvdv}{kT \left( 1 + \frac{\langle E^2 \rangle}{E_c^2} \right)} \right\}, \quad (2)$$

where  $E_c = v\sqrt{3xmkt/2e^2}$ . In the solar core being  $E$  not too larger than  $E_c$ , the distribution differs slightly from the Maxwellian. Crucial quantity is the elastic collision cross section is the enforced elastic Coulomb cross section  $\sigma_0 = 2\pi(\alpha r_0)^2$  where  $r_0$  is the inter-particle distance,  $\alpha$  is related to the pair-correlation function  $g(R, t)$ . The stationary (metastable) distribution (2) for the solar interior can be written as a function of the kinetic energy  $\epsilon_p$

$$f(\epsilon_p) = N \exp \left[ - \frac{\epsilon_p}{kT} - \delta \left( \frac{\epsilon_p}{kT} \right)^2 \right], \quad (3)$$

where the deformation parameter  $\delta = (1 - q)/2$  can be written as [8]

$$|\delta| \approx \frac{\sigma_0^2}{3\langle \sigma_d^2 \rangle} = 12\alpha^4 \Gamma^2 \ll 1. \quad (4)$$

A reasonable evaluation of  $\alpha$  gives:  $\alpha = 0.55$ , with  $\Gamma \sim 0.1$  and we obtain  $q = 0.990$  ( $\delta = 0.005$ ). In the next section we will see as such a small deviation of the MB distribution can be very relevant in several nuclear astrophysical applications.

Among the others, let us mention few problems where we can find signals of the presence of deviations from the MB distribution. Their solutions can be achieved by means of modified (or generalized) rates calculated by means of deformed distributions. We quote: A) Solar neutrino fluxes; B) Jupiter energy production; C) Atomic radiative processes in electron nuclear plasmas; D) Abundance of Lithium; E) Temperature dependence of modified CNO nuclear reaction rates and resonant fusion reactions. A detailed discussion of the problems can be found in Refs. [8, 9].

### 3. RELATIVISTIC HEAVY-ION COLLISIONS

In the last years, there was a growing interest to nuclear scattering and high energy physics applications of non-extensive statistics effects due to non-ideal many-body interactions.

In different pioneer works Ion and Ion [10] have obtained entropic lower bound for quantum scattering of spinless particles in the framework of Tsallis

thermostatistics. In Ref. [11], the authors have shown experimental evidence for non-extensive quantum statistical behavior in hadron-hadron scattering. As stated by the authors, this behavior can be interpreted as an indirect manifestation of the strong-coupling long-range regime in QCD.

Furthermore, several authors outline the possibility that experimental observations in relativistic heavy-ion collisions can reflect non-extensive features during the early stage of the collisions and the thermalization evolution of the system [12–16].

It is common opinion that hadrons dissociate into a plasma of their elementary constituents, quarks and gluons (QGP), at density several times the nuclear matter density and at temperature above few hundreds MeV (typically above 200 MeV), which is the critical temperature  $T_c$  of transition from the QGP phase to the hadronic gas phase. Such a QGP can be found in: early universe, dense and hot stars, neutron stars, nucleus-nucleus high energy collisions where heavy ions are accelerated to relativistic energies to collide.

After collision, a fireball is created which may be the QGP. The plasma expands, cools, freezes-out into hadrons (for instance pions), photons, leptons that are detected and analysed. Because interactions among quarks and gluons become weak at small distance or high energy, we usually expect that QGP is a weakly interacting plasma considered as an ideal one which can be described by perturbative QCD. However, this is rigorously true only at very high temperature ( $T > T_c$ ) while at the order of the critical temperature (that corresponds approximately to the energy scale of the SPS-Cern experiments) and in the hadronization phase there are strong non-perturbative QCD effects.

### 3.1. NON-IDEAL QGP PLASMAS AND KINETIC ASSUMPTIONS TOWARDS THE EQUILIBRIUM

The quark-gluon plasma close to the critical temperature is a strongly interacting system. In fact, following Ref. [12, 17, 18], the color-Coulomb coupling parameter of the QGP is defined, in analogy with the one of the classical plasma, as

$$\Gamma \approx C \frac{g^2}{4\pi r_0 T}, \quad (5)$$

where  $C = 4/3$  or  $3$  is the Casimir invariant for the quarks or gluons, respectively; for typical temperatures attained in relativistic heavy ion collisions,  $T \approx 200$  MeV,  $\alpha_s = g^2/(4\pi) = 0.2 \div 0.5$ , and  $r_0 \approx n^{-1/3} \approx 0.5$  fm ( $n$  being the particle density for an ideal gas of 2 quark flavors in QGP). Consequently, one obtains  $\Gamma \approx 1.5 - 5$  and the plasma can be considered to be in a non-ideal liquid phase [17, 18]. In these conditions, the generated QGP does not satisfy anymore the basic assumptions (BBGKY hierarchy) of a kinetic equation (Boltzmann or Fokker-Planck equation)

which describes a system toward the equilibrium. In fact, near the phase transition the interaction range is much larger than the Debye screening length and a small number of partons is contained in the Debye sphere [12, 18]. Therefore, the collision time is not much smaller than the mean time between collisions and the interaction is not local. The binary collisions approximation is not satisfied, memory effects and long-range color interactions give rise to the presence of non-Markovian processes in the kinetic equation, thus affecting the thermalization process toward equilibrium as well as the standard equilibrium distribution.

#### 4. RELATIVISTIC NON-EXTENSIVE KINETIC EQUATIONS

In order to study from a phenomenological point of view experimental observables in relativistic heavy-ion collisions, we can introduce the basic macroscopic variables in the language of relativistic kinetic theory following the Tsallis' prescriptions for the non-extensive statistical mechanics. In this framework the particle (four-vector) flow can be generalized as [30]

$$N^\mu(x) = \frac{1}{Z_q} \int \frac{d^3 p}{p^0} p^\mu f(x, p), \quad (6)$$

and the energy-momentum flow as

$$T^{\mu\nu}(x) = \frac{1}{Z_q} \int \frac{d^3 p}{p^0} p^\mu p^\nu [f(x, p)]^q, \quad (7)$$

where we have set  $\hbar = c = 1$ ,  $x \equiv x^\mu = (t, \mathbf{x})$ ,  $p \equiv p^\mu = (p^0, \mathbf{p})$  and  $p^0 = \sqrt{\mathbf{p}^2 + m^2}$  is the relativistic energy. In the above  $Z_q = \int d\Omega [f(x, p)]^q$  is the non-extensive partition function,  $d\Omega$  stands for the corresponding phase space volume element and  $q$  is the deformation parameter. The limit  $q \rightarrow 1$  corresponds to ordinary statistics. The four-vector  $N^\mu = (n, \mathbf{j})$  contains the probability density  $n = n(x)$  (which is normalized to unity) and the probability flow  $\mathbf{j} = \mathbf{j}(x)$ . The energy-momentum tensor contains the normalized  $q$ -mean expectation value<sup>1</sup> of the energy density, as well as the energy flow, the momentum and the momentum flow per particle.

On the basis of the above definitions, one can show that it is possible to obtain a generalized non-linear relativistic Boltzmann equation [30]

<sup>1</sup> The  $q$ -mean expectation value is defined as [27, 30]:

$$\langle O(x) \rangle_q = \int d^3 p O(x, p) [f(x, p)]^q / \int d\Omega [f(x, p)]^q. \quad (8)$$

$$p^\mu \partial_\mu [f(x, p)]^q = C_q(x, p), \quad (9)$$

where the function  $C_q(x, p)$  implicitly defines a generalized non-extensive collision term

$$C_q(x, p) = \frac{1}{2} \int \frac{d^3 p_1}{p_1^0} \frac{d^3 p'}{p'^0} \frac{d^3 p'_1}{p'^0_1} \{h_q[f', f'_1] W(p', p'_1 | p, p_1) - h_q[f, f_1] W(p, p_1 | p', p'_1)\}. \quad (10)$$

Here  $W(p, p_1 | p', p'_1)$  is the transition rate between a two-particle state with initial four-momenta  $p$  and  $p_1$  and a final state with four-momenta  $p'$  and  $p'_1$ ;  $h_q[f, f_1]$  is the  $q$ -correlation function relative to two particles in the same space-time position but with different four-momenta  $p$  and  $p_1$ , respectively. Such a transport equation conserves the probability normalization (number of particles) and is consistent with the energy-momentum conservation laws. The collision term contains a generalized expression of the molecular chaos and for  $q > 0$  implies the validity of a generalized  $H$ -theorem, if the following, non-extensive, local four-density entropy is assumed

$$S_q^\mu(x) = -k_B \int \frac{d^3 p}{p^0} p^\mu f[(x, p)]^q [\ln_q f(x, p) - 1], \quad (11)$$

where we have used the definition  $\ln_q x = (x^{1-q} - 1)/(1 - q)$ . At equilibrium, the solution of the above Boltzmann equation is a relativistic Tsallis-like (power law) distribution and can be written as

$$f^{eq}(p) = \frac{1}{Z_q} \left[ 1 - (1 - q) \frac{p^\mu U_\mu}{k_B T} \right]^{1/(1-q)}. \quad (12)$$

In the limit  $q \rightarrow 1$ , Eq. (12) reduces to the standard relativistic equilibrium Jüttner distribution.

The above relations represent the basic framework in which, in the next section, will be studied the net-baryon rapidity distribution near equilibrium.

#### 4.1. NET-BARYON RAPIDITY DISTRIBUTION

The energy loss of colliding nuclei is a fundamental quantity in order to determine the energy available for particle production in heavy-ion collisions. Since the baryon number is conserved and rapidity distributions are only affected by rescattering in the late stages of the collision, the measured net-baryon ( $B - \bar{B}$ ) distribution retains information about the energy loss and allows one to obtain the

degree of nuclear stopping [19, 20]. Recent results for net-proton rapidity spectra in central Au+Au collisions at RHIC [21] show an unexpectedly large rapidity density at midrapidity in comparison with analogous spectra at lower energy at SPS [22] and AGS [23]. As outlined from different authors, such spectra can reflect non-equilibrium effects even if the energy dependence of the rapidity spectra is not very well understood [21, 24, 25].

In order to study the rapidity spectra, it is convenient to separate the kinetic variables into their transverse and longitudinal components, the latter being related to the rapidity  $y$ . If we assume that the particle distribution function  $f(y, m_{\perp}, t)$ , at fixed transverse mass  $m_{\perp} = \sqrt{m^2 + p_{\perp}^2}$ , is not appreciably influenced by the transverse dynamics (which is considered in thermal equilibrium), the non-linear Fokker-Planck equation in the rapidity space  $y$  can be written as

$$\frac{\partial}{\partial t}[f(y, m_{\perp}, t)] = \frac{\partial}{\partial y} \left[ J(y, m_{\perp})[f(y, m_{\perp}, t)] + D \frac{\partial}{\partial y} [f(y, m_{\perp}, t)]^{\mu} \right], \quad (13)$$

where  $D$  and  $J$  are the diffusion and drift coefficients, respectively.

Tsallis and Bukman [26, 27] have shown that, for linear drift, the time dependent solution of the above equation is a Tsallis (non-relativistic) distribution with  $\mu = 2 - q$  and that a value of  $q \neq 1$  implies anomalous diffusion, *i.e.*,  $[y(t) - y_M(t)]^2$  scales like  $t^{\alpha}$ , with  $\alpha = 2/(3 - q)$ . For  $q < 1$ , the above equation implies anomalous subdiffusion, while for  $q > 1$ , we have a superdiffusion process in the rapidity space. Let us note that a similar approach, within a linear and non-linear Fokker-Planck equation, has been previously studied in Ref. [28] involving directly the time evolution of the rapidity distribution instead of the particle distribution function  $f(y, m_{\perp}, t)$ , as in the Eq. (13). The two approaches are equivalent only if the particle distribution is completely decoupled in the transverse and in the longitudinal coordinates and the drift coefficient  $J$  does not depend on transverse momentum. We claim that the choice of the diffusion and the drift coefficients plays a crucial rôle in the solution of the above non-linear Fokker-Planck equation (13). Such a choice influences the time evolution of the system and its equilibrium distribution [29].

We are going to show that by generalizing the Brownian motion in a relativistic framework, the standard Einstein relation is satisfied and anomalous diffusion emerges in a natural way from the non-linearity of the Fokker-Planck equation [30]. In fact, by imposing the validity of the Einstein relation for Brownian particles and setting henceforward the Boltzmann constant  $k_B$  to unity, we can generalize to the relativistic case the standard expressions of diffusion and drift coefficients as follows

$$D = \gamma T, \quad J(y, m_{\perp}) = \gamma m_{\perp} \sinh(y) \equiv \gamma p_{\parallel}, \quad (14)$$

where  $p_{\parallel}$  is the longitudinal momentum,  $T$  is the temperature and  $\gamma$  is a common constant. Let us remark that the above definition of the diffusion and drift coefficients appears as the natural generalization to the relativistic Brownian case in the rapidity space. The drift coefficient which is, as usual, linear in the longitudinal momentum  $p_{\parallel}$  becomes non-linear in the rapidity coordinate.

It is easy to see that the above coefficients give us the Boltzmann stationary distribution in the linear case ( $q = \mu = 1$ ), while the equilibrium solution  $f^{eq}(y, m_{\perp})$  of Eq. (13), with  $\mu = 2 - q$ , is a Tsallis-like distribution [27, 30, 14, 31] with the relativistic energy  $E = m_{\perp} \cosh(y)$

$$f^{eq}(y, m_{\perp}) = [1 - (1 - q)m_{\perp} \cosh(y)/T]^{1/(1-q)}. \quad (15)$$

Out of equilibrium the rapidity distribution at fixed time can be obtained by means of numerical integration of Eq. (13) with delta function initial conditions depending upon the value of the experimental projectile rapidities. The rapidity distribution at fixed time is then obtained by numerical integration over the transverse mass  $m_{\perp}$  as follows

$$\frac{dN}{dy}(y, t) = c \int_m^{\infty} m_{\perp}^2 \cosh(y) f(y, m_{\perp}, t) dm_{\perp}, \quad (16)$$

where  $m$  is the mass of the considered particles and  $c$  is the normalization constant, fixed by the experimental data. The rapidity spectra calculated from Eq. (16) will ultimately depend on two parameters: the ‘‘interaction’’ time  $\tau_{int} = \gamma t$  and the anomalous diffusion parameter  $q$ .

In Figs. 1 and 2 we plot the numerical solution of Eqs. (13) and (16) at different interaction times  $\tau_{int}$  in the linear case ( $q = 1$ ) and in the non-linear case, with  $q = 1.25$ , keeping the same initial conditions. In comparing Fig. 1 with Fig. 2, we can observe that the rapidity spectra appear to be broader in the non-linear case. This is a consequence of the anomalous (super)diffusion process implied in the time evolution of Eq. (13) and in the nature of the power law distribution function which, for  $q > 1$ , enhances the probability to find particles at high rapidity values.

In Fig. 3, we report the obtained rapidity distribution (full line) for the net proton production ( $p - \bar{p}$ ) compared with the experimental data of RHIC (Au + Au at  $\sqrt{s_{NN}} = 200$  GeV, [21]), SPS (Pb + Pb at  $\sqrt{s_{NN}} = 17.3$  GeV, [22]) and AGS (Au + Au at  $\sqrt{s_{NN}} = 5$  GeV, [23]). The parameters employed for the three curves are:  $q = 1.485$  with  $\tau_{int} = 0.47$  for RHIC,  $q = 1.235$  with  $\tau_{int} = 0.84$  for SPS and  $q = 1.09$  with  $\tau_{int} = 0.95$  for AGS, respectively. We notice that, although  $q$  and  $\tau_{int}$  appear, in principle, as independent parameters, in fitting the data they are not. Indeed, we can see that only in the non-linear case ( $q \neq 1$ ) there exists one and

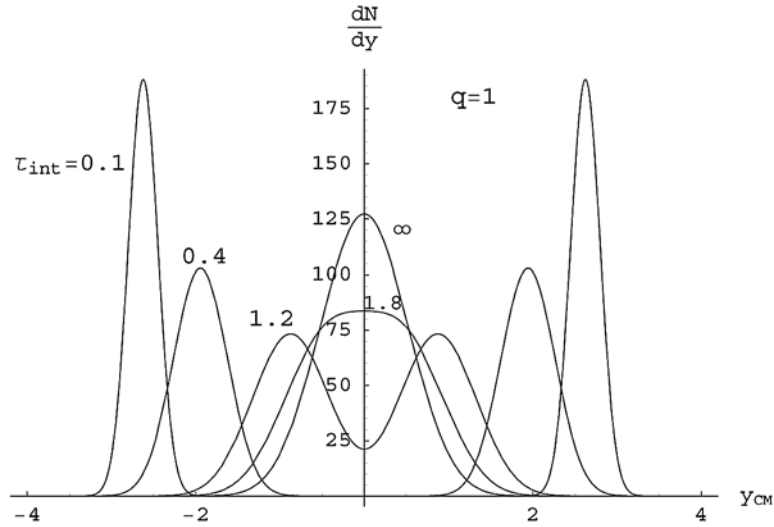


Fig. 1 – Numerical solution of Eqs. (13) and (16) at different interaction times  $\tau_{int}$  in the linear case ( $q = 1$ ).

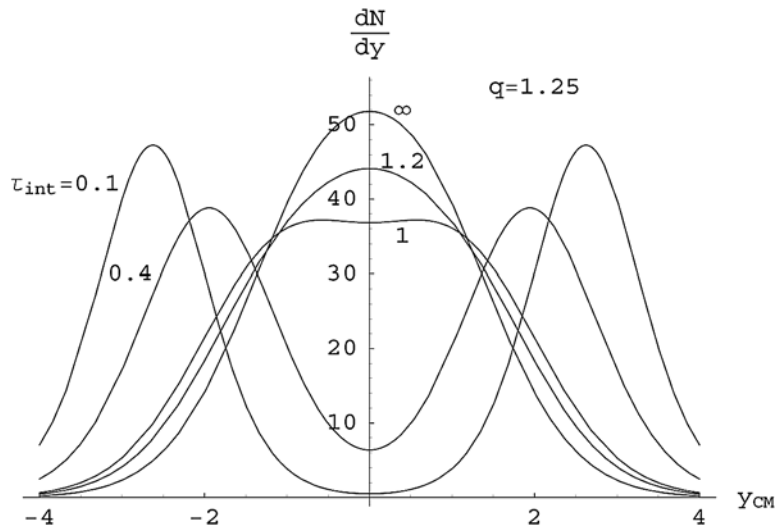


Fig. 2 – The same of Fig. 1 but in the non-linear case with  $q = 1.25$ .

only one (finite) time  $\tau_{int}$  for which the obtained rapidity spectrum well reproduces the broad experimental shape. On the contrary, for  $q = 1$ , no value of  $\tau_{int}$  can be found, which allows to reproduce the data. We obtain a remarkable agreement with the experimental data by increasing the value of the non-linear deformation parameter  $q$  as the beam energy increases. At AGS energy, the non-extensive statistical effects are negligible and the spectrum is well reproduced within the

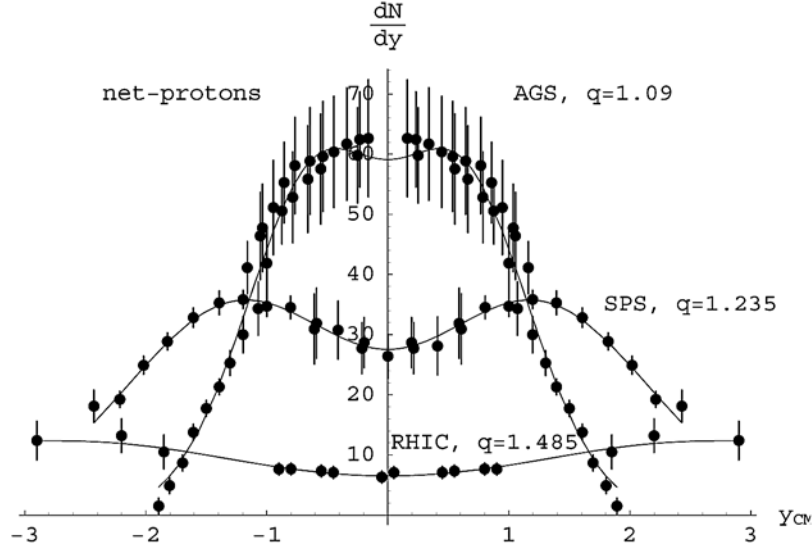


Fig. 3 – Rapidity spectra for net proton production ( $p - \bar{p}$ ) at RHIC (Au + Au at  $\sqrt{s_{NN}} = 200$  GeV, BRAHMS data), SPS (Pb + Pb at  $\sqrt{s_{NN}} = 17.3$  GeV, NA49 data) and AGS (Au + Au at  $\sqrt{s_{NN}} = 5$  GeV, E802, E877, E917).

standard quasi-equilibrium linear approach. At SPS energy, non-equilibrium effects and non-linear evolution become remarkable ( $q = 1.235$ ) and such effects are even more evident for the very broad RHIC spectra ( $q = 1.485$ ).

From a phenomenological point of view, we can read the larger value of the anomalous diffusion parameter  $q$  for the RHIC data, corresponding to non-linear anomalous (super)diffusion, as a signal of the non-ideal nature of the plasma formed at a temperature larger than the critical one. Strongly coupled non-ideal plasma is generated at energy densities corresponding to the order of the critical phase transition temperature and in such a regime we find, in our macroscopic approach, strong deviations from the standard thermostatics. At much higher energy, such as LHC, we can expect a minor relevance of such non-ideal effects since the considerable energy density reached is far above the critical one. However, an anomalous diffusion behavior should still affect the time evolution process toward the equilibrium due to long range color magnetic forces which remain unscreened (in leading order) at all temperatures.

## REFERENCES

1. G. L. Sewell, Phys. Rep. **57**, 307 (1980).
2. V. Latora, A. Rapisarda, C. Tsallis, Phys. Rev. **E64**, 056134 (2001).
3. M. Montemurro, F. Tamarit, C. Anteneodo, Phys. Rev. **E67**, 031106 (2003).

4. F. Ferro, A. Lavagno, P. Quarati, *Phys. Lett.* **A336**, 370 (2005).
5. M. Gell-Mann, C. Tsallis Eds., *Nonextensive entropy-Interdisciplinary applications*, Oxford University Press, Oxford, 2004.
6. Y. S. Weinstein, S. Lloyd, C. Tsallis, *Phys. Rev. Lett.* **89**, 214101 (2002).
7. G. Ananos, C. Tsallis, *Phys. Rev. Lett.* **93**, 020601 (2004).
8. A. Lavagno, P. Quarati, *Phys. Lett.* **B498**, 291 (2001).
9. F. Ferro, A. Lavagno, P. Quarati, *Physica* **A340**, 477 (2004);  
F. Ferro, A. Lavagno, P. Quarati, *Eur. Phys. J.* **A21**, 529 (2004).
10. D. B. Ion, M. L. D. Ion, *Phys. Rev. Lett.* **81**, 5714 (1998);  
*Phys. Rev. Lett.* **83**, 463 (1999);  
*Phys. Rev.* **E60**, 5261 (1999).
11. D. B. Ion, M. L. D. Ion, *Physica* **A340**, 501 (2004).
12. W. M. Alberico, A. Lavagno, P. Quarati, *Eur. Phys. J.* **C12**, 499 (2000);  
W. M. Alberico, A. Lavagno, P. Quarati, *Nucl. Phys.* **A680**, 94c (2001).
13. G. Wilk, Z. Włodarczyk, *Phys. Rev. Lett.* **84**, 2770 (2000).
14. D. B. Walton, J. Rafelski, *Phys. Rev. Lett.* **84**, 31, (2000).
15. I. Bediaga, E. M. F. Curado, J. M. de Miranda, *Physica* **A286**, 156 (2000).
16. C. Beck, *Physica* **A286**, 164 (2000).
17. A. Peshier, W. Cassing, *Phys. Rev. Lett.* **94**, 172301 (2005).
18. M. H. Thoma, *J. Phys.* **G31**, L7, (2005).
19. B. Biedroń, W. Broniowski, *nucl-th/0610083*.
20. I. Arsene *et al.* (BRAHMS Collaboration), (2007) submitted to *Phys. Lett.* **B**, S. J. Sanders (BRAHMS Collaboration), *nucl-ex/0701076*.
21. I. G. Bearden *et al.* (BRAHMS Collaboration), *Phys. Rev. Lett.* **93**, 102301 (2004).  
B. I. Abelev *et al.* (STAR Collaboration) *nucl-ex/060921*.
22. H. Appelshäuser *et al.* (NA49 Collaboration), *Phys. Rev. Lett.* **82**, 2471 (1999).
23. B. B. Back *et al.* (E917 Collaboration), *Phys. Rev. Lett.* **86**, 1970 (2001);  
L. Ahle *et al.* (E802 Collaboration), *Phys. Rev.* **C60**, 064901 (1999);  
J. Barette *et al.* (E977 Collaboration), *Phys. Rev.* **C62**, 024901 (2000).
24. B. I. Abelev *et al.* (STAR Collaboration), *nucl-ex/0609021*.
25. M. Biyajima *et al.*, *Prog. Theor. Phys. Suppl.* **153**, 344 (2004).
26. C. Tsallis, D. J. Bukman, *Phys. Rev.* **E54**, R2197 (1996).
27. M. Gell-Mann, C. Tsallis, eds., *Nonextensive Entropy: Interdisciplinary Applications*, Oxford University Press, New York, 2004.
28. G. Wolschin, *Phys. Rev.* **C69**, 024906 (2004);  
*Europhys. Lett.* **74**, 29 (2006).
29. L. Ravagli, R. Rapp, *hep-ph/0705.0021*.
30. A. Lavagno, *Phys. Lett.* **A301**, 13 (2002).
31. T. S. Biró, A. Jakovác, *Phys. Rev. Lett.* **94**, 132302 (2005);  
T.S. Biró, G. Purcsel, *Phys. Rev. Lett.* **95**, 162302 (2005).